

Figure S1

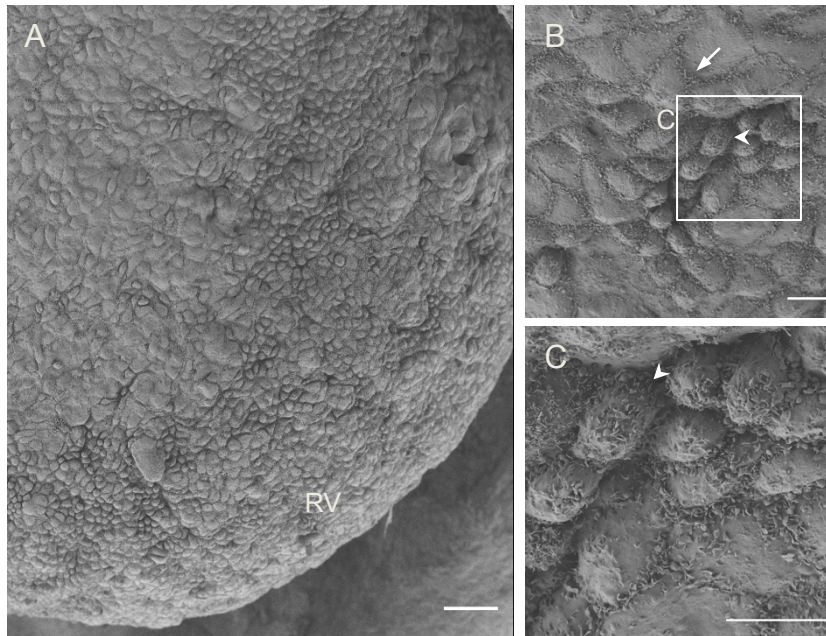


Figure S1. Cells with epithelial morphology and mesenchymal morphology within the embryonic epicardium. (A): the dorsal surface of an E13.5 embryonic heart, showing epicardial cells with different morphologies. (B): Magnified epicardium focusing on large and flat, epithelial-like cells (white arrow) and small, pillar-shaped, dispersed mesenchymal-like cells (white arrowhead). (C): magnified view of the inset box from (B). Scale bars: A, 50 μm . B, C: 10 μm . RV: right ventricle.

Figure S2

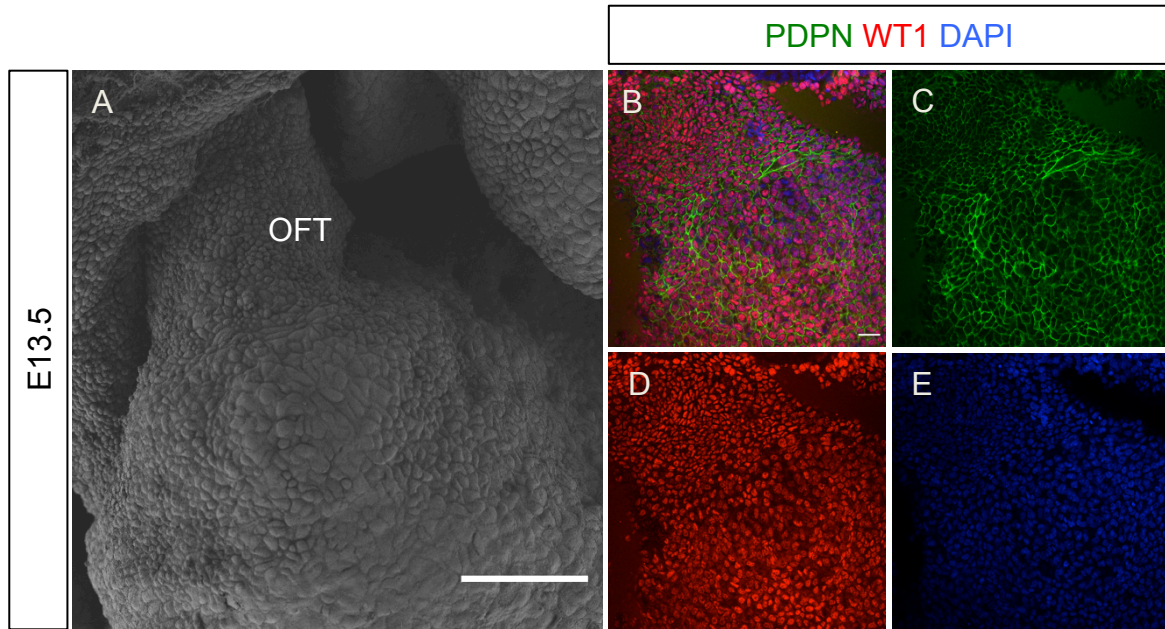


Figure S2. Morphological differences between epicardial cells in the OFT. (A): the OFT of an E13.5 heart under SEM: note the presence of distinct small, round cells and large, flat cells. (B-E), Whole-mount immunofluorescent staining of E13.5 for podoplanin (PDPN; green) and WT1 (red). Scale bars: 50 μ m. OFT: outflow tract.

Figure S3

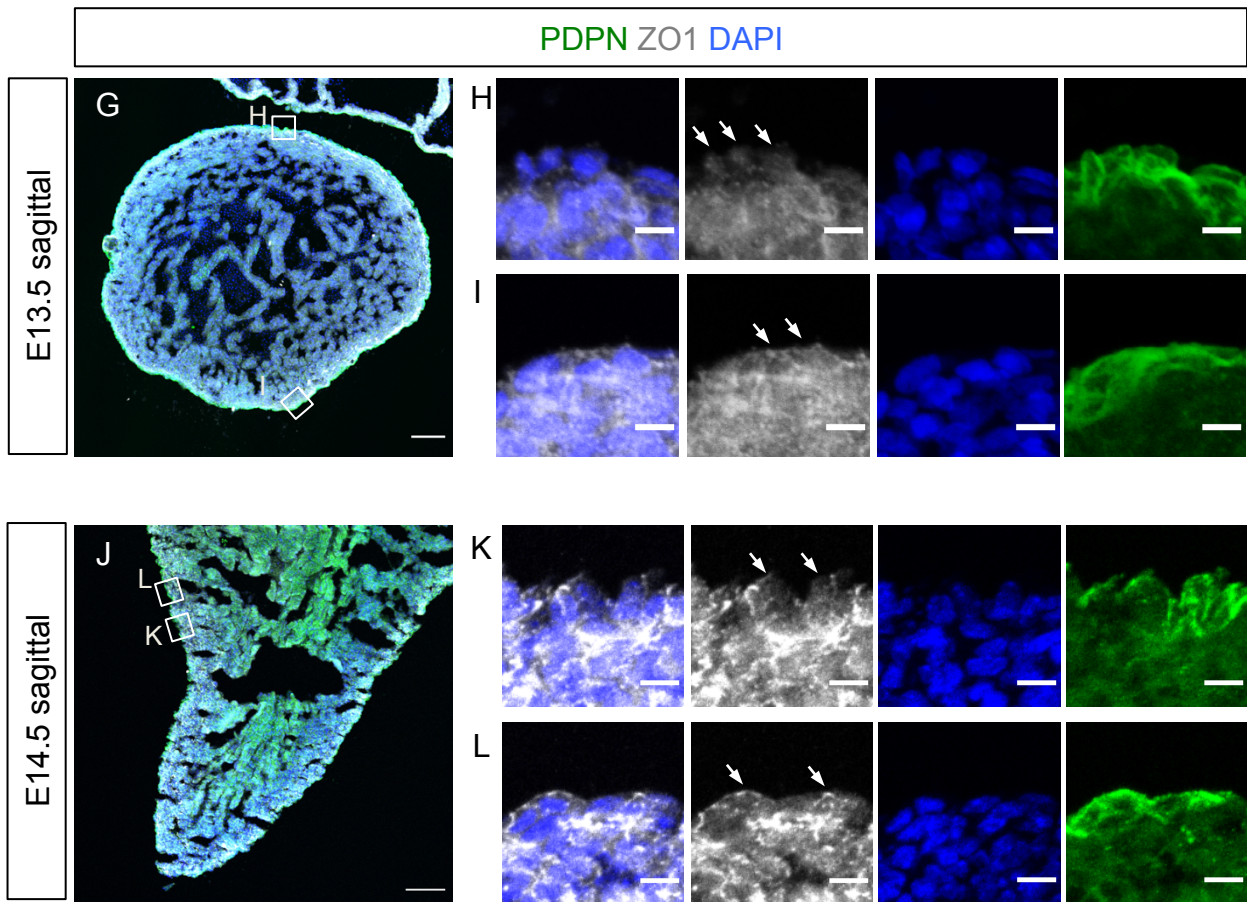
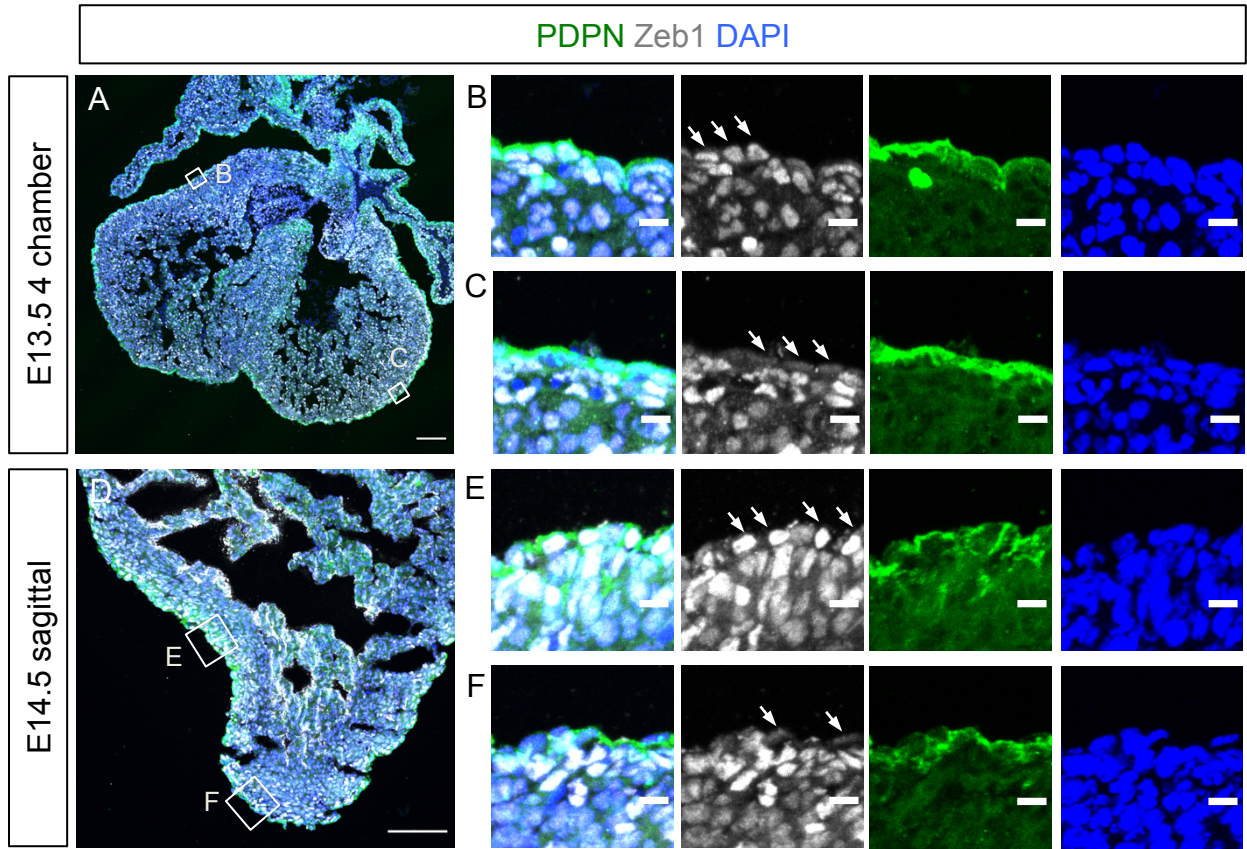


Figure S3. Heterogenous EMT status of epicardial cells. (A-F): immunofluorescent staining of ZEB1 (white), Podoplanin (PDPN; green) and DAPI (blue) of a section from a E13.5 heart (A) and a section from E14.5 heart (D). (B and C) are magnified view from the inset boxes in (A). (E and F) are magnified view from the inset boxes in (D) Epicardial cells express high level of Zeb1 (B, E white arrows) and low level of Zeb1 (C, F, white arrows). (G-L): immunofluorescent staining of ZO1 (white), Podoplanin (green) and DAPI (blue) of a section from a E13.5 heart (G) and a section from a E14.5 heart (J). (H and I) are magnified view from the inset boxes in (A). (K and L) are magnified view from the inset boxes in (J). In (H and K), epicardial cells bear low and discontinuous ZO1 expression (white arrows). In (I and L), ZO1 is detected in cell junctions and apical side (white arrows). Scale bars: A, D, G, J: 50 μm . B, C, E, F, H, I, K, L: 10 μm .

Figure S4

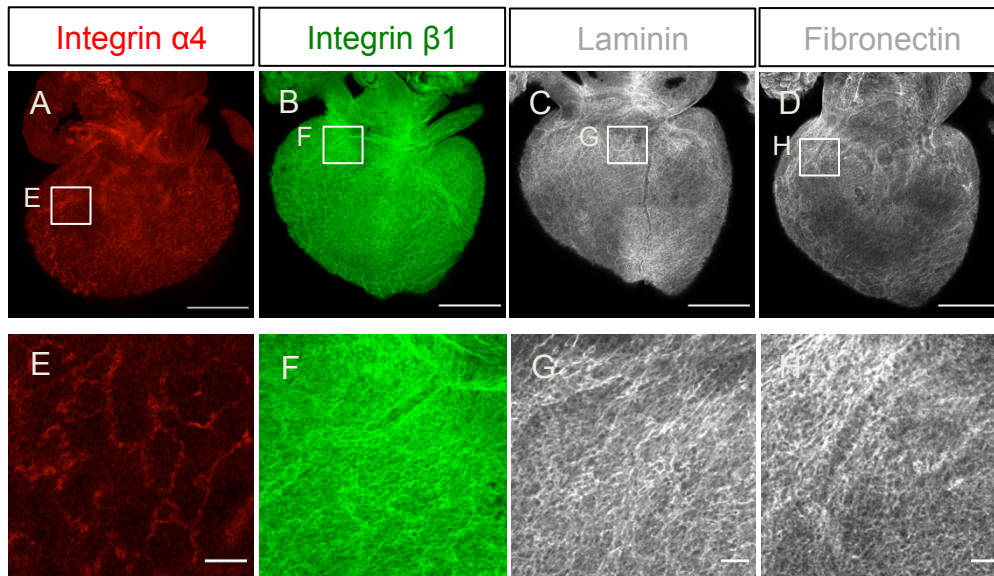


Figure S4. Expression of extracellular matrix components within the embryonic epicardium. (A-D). Wholemount immunofluorescent staining of integrin α 4 (red), integrin β 1 (green), laminin (white) and fibronectin (white) on E14.5 embryonic hearts. E-H: magnified view of the inset boxes from A-D. Scale bars: A-D, 500 μ m. E-H: 50 μ m.

Figure S5

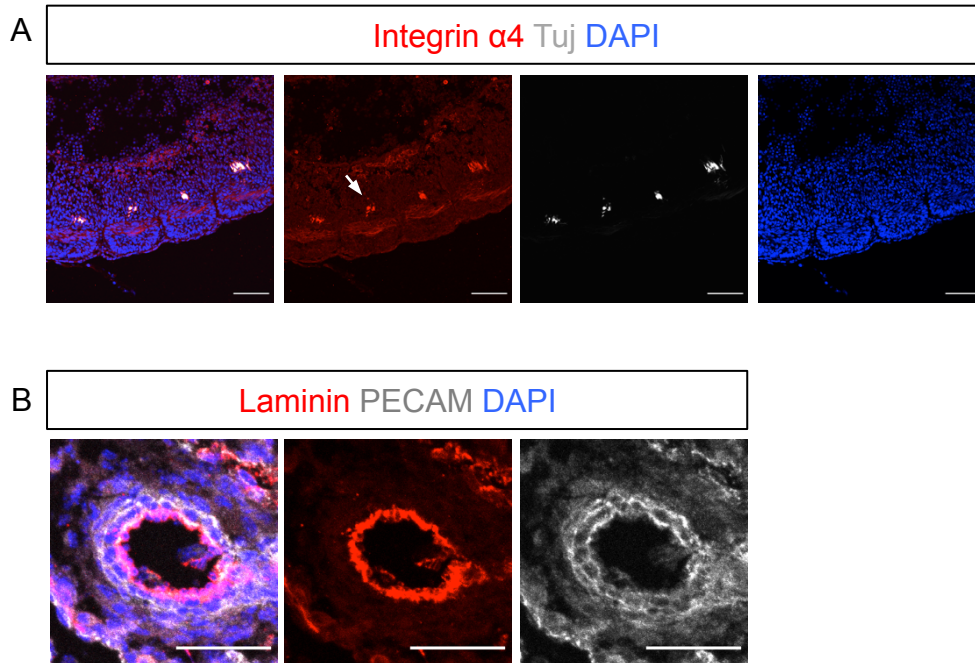


Figure S5. Validation of integrin α 4 and laminin antibodies. (A): Immunofluorescent staining of Integrin α 4 (red), Neuronal β -tubulin (TuJ1) and DAPI (blue) of a section from a E10.5 embryo. Integrin α 4 overlaps with TuJ in somites. (B): Immunofluorescent staining of laminin (red) and PECAM (white) of a blood vessel. Scale bars: 50 μ m.

Figure S6

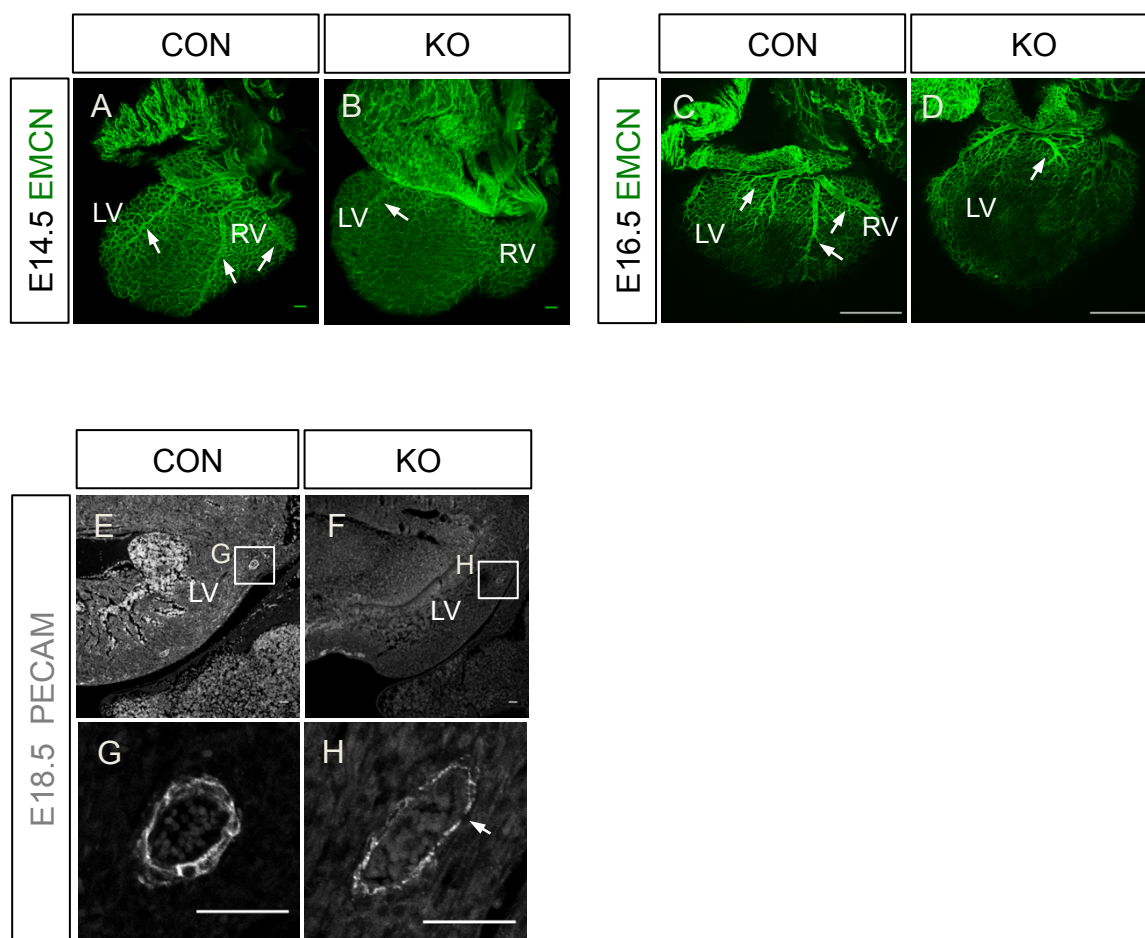


Figure S6. Coronary vasculature defects in agrin KO hearts. (A-D), whole-mount immunofluorescent staining for EMCN (green) of E14.5 (A, B) and E16.5 (C, D) littermate controls (A, C) and agrin KO hearts (B, D) labeling the coronary vasculature. Dorsal aspects are presented. Note the clearly defined and extended major vessels in the control heart (white arrows in A) which are virtually absent in the KO heart (white arrow in B). In E16.5 agrin KO heart, the main vessels are truncated (white arrows in D). (E-H), immunofluorescent staining on sections from E18.5 litter control hearts (E, G) and agrin KO (F, H) hearts for PECAM labeling endothelial cells. (G, H) are magnified views from the inset boxes in (E, F) showing a transverse section of a main coronary vessel. Note the weak and discontinuous PECAM staining in the agrin KO heart indicative of vessel instability (white arrow in H). Scale bars: A, B: 100 μ m, C, D: 500 μ m. E-H: 50 μ m.

Figure S7

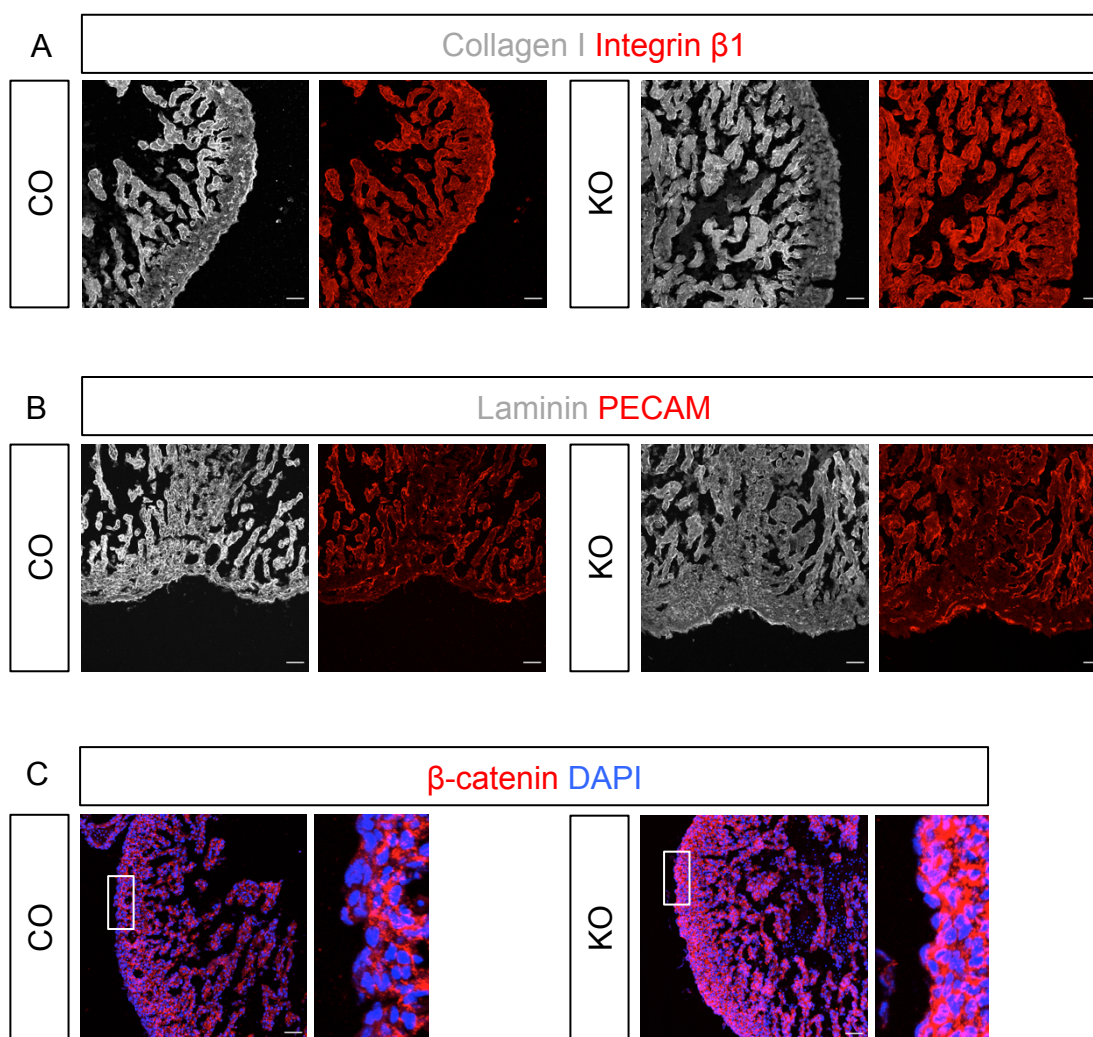


Figure S7. ECM components are abnormally deposited in agrin KO myocardium. Immunofluorescent staining of Collagen I (A, white), Integrin β 1 (A, red), Laminin (B, white), PECAM (B, red) and β -catenin (C, red) in serial sections of embryonic hearts of E14.5 littermate control and agrin KO. Scale bars: 50 μ m.

Figure S8

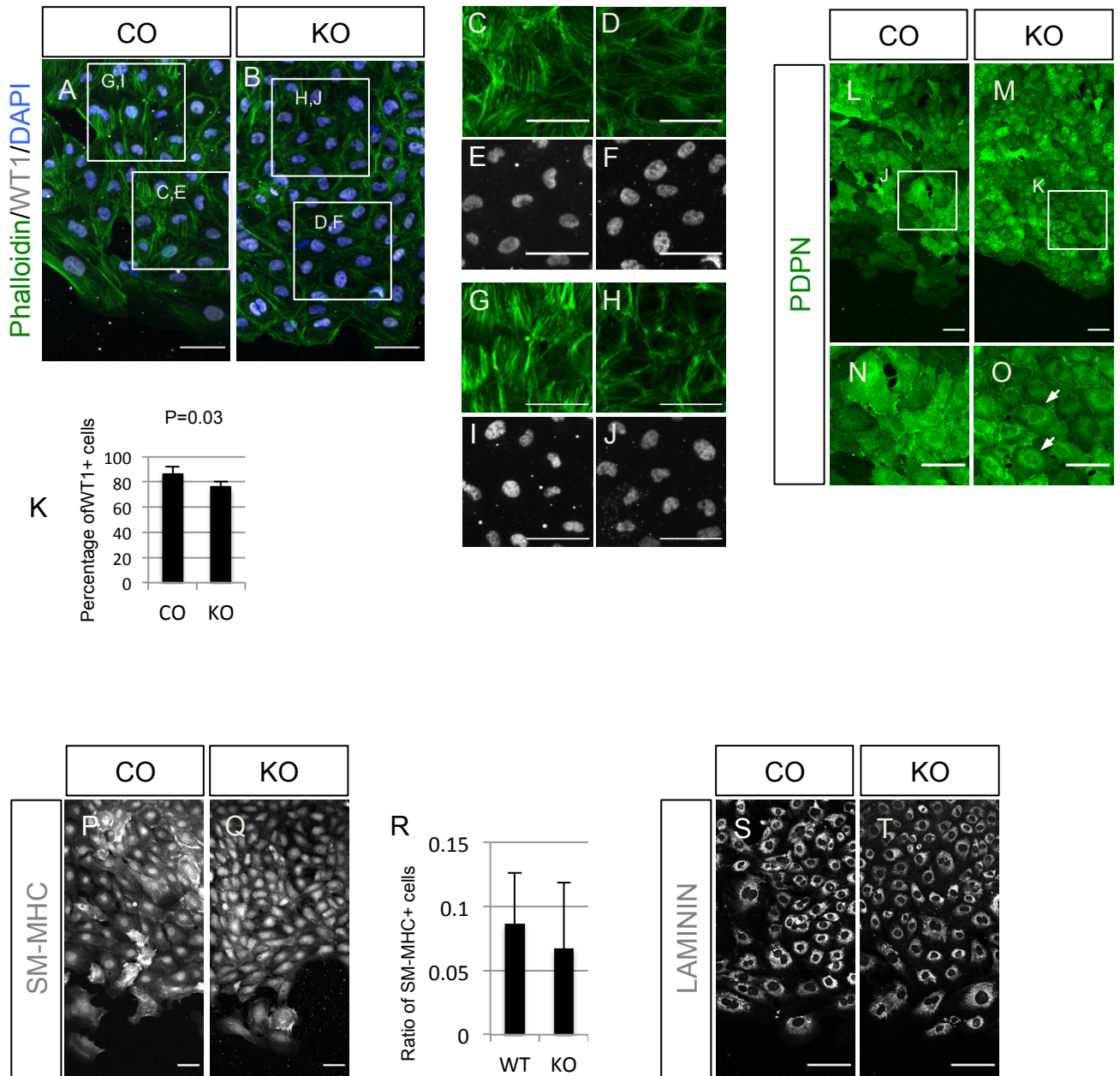


Figure S8. Migration and ECM defects in epicardium-derived cells from agrin-KO explants.

(A-B) Immunofluorescent staining of epicardium-derived cells migrated away from E11.5 explants of littermate control and agrin KO for cell stress fibers (phalloidin, green), WT1 (white) and nuclei (DAPI). (C and E), (G and I) are magnified view of the inset boxes in (A). (D and F), (H and J) are magnified view of the inset boxes in (B). (K) Quantification of WT1⁺ cells in control explant-derived and agrin KO derived epicardial cells. Data represent mean \pm SEM. N=4 hearts per group. Significant differences (P-value) were calculated using an unpaired, two-tailed Student's *t*-test. (L, M) Immunofluorescent staining for podoplanin (green) in epicardium-derived cells from control and agrin KO explants. (N and O) are magnified view of the box in (L) and (M). Epicardial cells derived from the agrin KO explant showed weak podoplanin on the cell surface, especially in peri-nuclear regions (white arrows in O). (P, Q, S, T) Immunofluorescent staining for SM-MHC (P, Q) and Laminin (S, T) of epicardial cells from littermate control (P, S) and agrin KO explants (Q, T). (R): quantification of SM-MHC-positive cells in total explant-derived epicardial cells. Data represent mean \pm S.E.M.; n=4 independent samples per group. Significant differences (P-value) were calculated using an unpaired, two-tailed Student's *t*-test. All scale bars: 50 μ m.

Figure S9

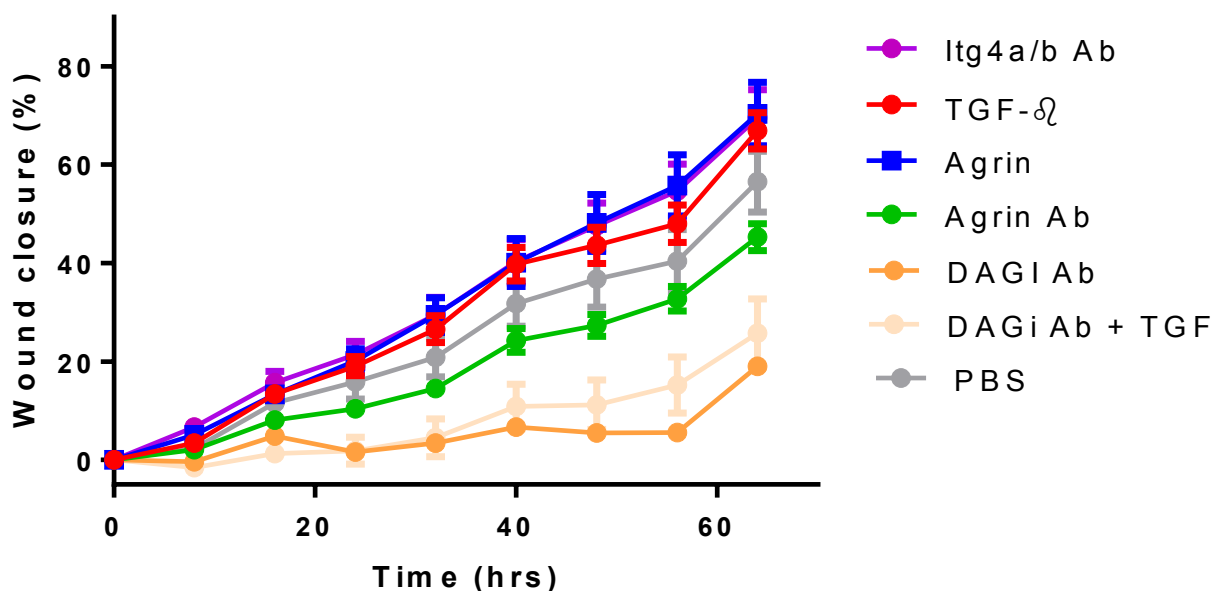


Figure S9. Agrin enhances the migration of mouse epicardial cells. Immortalised mouse epicardial cells were cultured for 64 hours with the indicated reagents and the wound closure was evaluated. Data represent mean \pm SEM; n=12 independent treatments per group. Significant differences (P value) were calculated using one way ANOVA. Agrin treatment significantly increased the rate of 75% wound closure compared to untreated (PBS) and even TGF β -treatment.

Figure S10

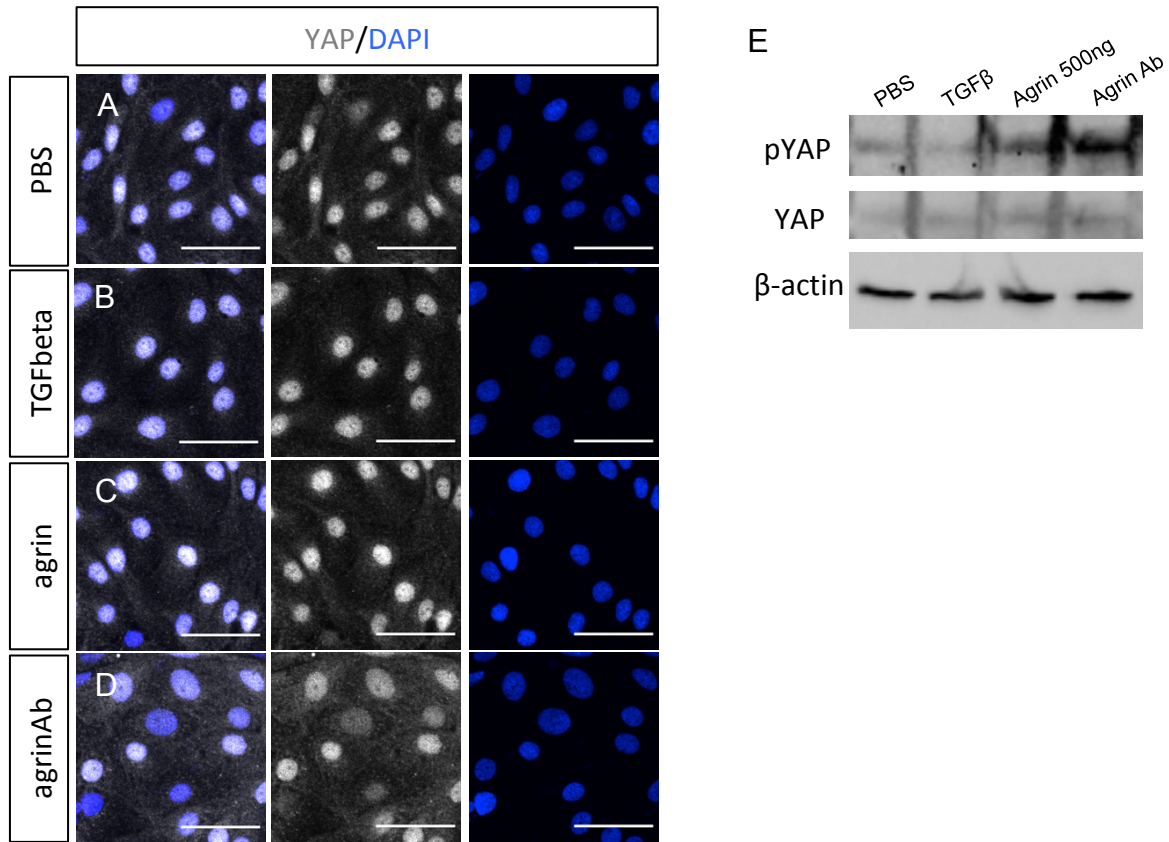


Figure S10. Blocking agrin inhibits YAP in epicardial cells. (A-D) Immunofluorescent staining of YAP (white) and DAPI (blue) in hESC-derived epicardial-like cells. (E) Western blot showing agrin and agrin antibody enhanced the expression of phosphorylated YAP. Scale bars: 10 μ m.

Table S1. Experimental models: organisms/strains

Mouse: <i>Agrin^{fl/fl}: B6.129-Agrn^{tm1Rwb}/J</i>	The Jackson Laboratory	JAX: 031788
Mouse: <i>PGK-Cre: B6.C-Tg(Pgk1-cre)1Lni/CrsJ</i>	The Jackson Laboratory	JAX: 021160
Mouse: <i>Wt1-CreERT2: WT1^{tm2(cre/ERT2)Wtp}/J</i>	The Jackson Laboratory	JAX: 010912
Mouse: <i>Wt1-GFPCre: Wt1^{tm1(EGFP/cre)}Wtp/J</i>	The Jackson Laboratory	JAX: 010911

Table S2. Antibodies

Mouse monoclonal anti-human agrin Alexa647(D2)	Santa Cruz (1:100)	Cat# Sc374117-AF647
Mouse monoclonal anti-agrin	EMD Millipore	Cat# MAB5204
Rabbit polyclonal anti-mouse beta-catenin	Abcam (1:250)	Cat# AF2727
Rabbit polyclonal anti-mouse collagen I	Abcam (1:200)	Cat# Ab34710
Rat polyclonal anti-mouse CD31 (clone MEC13.3)	Abcam	Cat# 550274
Goat monoclonal anti-mouse DAG1	Abcam (1:200)	Cat# Ab136665
Rat monoclonal anti-mouse EMCN (clone V.5C7)	Santa Cruz Biotech (1:50)	Cat# sc-53941
Rabbit polyclonal anti-mouse fibronectin	Abcam (1:200)	Cat# 23750
Rabbit polyclonal anti-human GM130	Invitrogen (1:200)	Cat# 95727
Rat monoclonal anti-mouse Integrin alpha4	BD Pharmingen (1:200)	Cat# 553314
Anti-integrin alpha4 (Natalizumab)	Absolute (1:100)	Cat# Ab00716-1.1
Rat monoclonal anti-mouse integrin beta1	EMD Millipore (1:200)	Cat# MAB1997
Rabbit polyclonal anti-mouse total laminin	Abcam (1:200)	Cat# Ab11575
Rabbit anti-mouse pFAK	Cell Signaling Technology (1:200)	Cat# 8556S
Rabbit polyclonal anti-mouse p-Histone H3 (Ser10)	Santa Cruz	Cat# Sc-56739
Hamster monoclonal anti-mouse podoplanin (clone 103-M40)	Fitzgerald (1:200)	Cat# 10R-P155A
Rabbit polyclonal anti-mouse WT1	Abcam(1:200)	Cat# Ab89901
Rabbit polyclonal anti-mouse YAP	Abcam(1:200)	Cat# Ab89901
Rabbit polyclonal anti-mouse YAP pY397	Abcam(1:200)	Cat# Ab89901
Rabbit polyclonal anti-mouse Zeb1	Abcam(1:200)	Cat# Ab89901
Rabbit polyclonal anti-mouse ZO1	Abcam(1:200)	Cat# Ab89901
Donkey anti-rat IgG Alexa Fluor 488	Thermofisher	Cat# A21208
Donkey anti-rat IgG Alexa Fluor 555	Abcam	Cat# Ab150154
Donkey anti-rabbit IgG Alexa Fluor 555	Thermofisher	Cat# A32794

Donkey anti-rabbit IgG Alexa Fluor 647	Thermofisher	Cat# A31573
Goat anti-hamster IgG Alexa Fluor 488	Thermofisher	Cat# A21110
Donkey anti-goat IgG Alexa Fluor 488	Thermofisher	Cat# A11055
Donkey anti-goat IgG Alexa Fluor 555	Abcam	Cat# Ab150134